Journal of Soils and Sediments (2022) 22:348–364
https://doi.org/10.1007/s11368-021-03107-6

SEDIMENTS, SEC 3 • HILLSLOPE AND RIVER BASIN SEDIMENT DYNAMICS • RESEARCH ARTICLE

High frequency un-mixing of soil samples using a submerged spectrophotometer in a laboratory setting—implications for sediment fingerprinting

Niels F. Lake[1,2] · Núria Martínez-Carreras[1] · Peter J. Shaw[2] · Adrian L. Collins[3]

Received: 18 May 2021 / Accepted: 4 November 2021 / Published online: 22 November 2021

Abstract

Purpose This study tests the feasibility of using a submersible spectrophotometer as a novel method to trace and apportion suspended sediment sources in situ and at high temporal frequency.

Methods Laboratory experiments were designed to identify how absorbance at different wavelengths can be used to un-mix artificial mixtures of soil samples (i.e. sediment sources). The experiment consists of a tank containing 40 L of water, to which the soil samples and soil mixtures of known proportions were added in suspension. Absorbance measurements made using the submersible spectrophotometer were used to elucidate: (i) the effects of concentrations on absorbance, (ii) the relationship between absorbance and particle size and (iii) the linear additivity of absorbance as a prerequisite for un-mixing.

Results The observed relationships between soil sample concentrations and absorbance in the ultraviolet visible (UV–VIS) wavelength range (200–730 nm) indicated that differences in absorbance patterns are caused by soil-specific properties and particle size. Absorbance was found to be linearly additive and could be used to predict the known soil sample proportions in mixtures using the MixSIAR Bayesian tracer mixing model. Model results indicate that dominant contributions to mixtures containing two and three soil samples could be predicted well, whilst accuracy for four-soil sample mixtures was lower (with respective mean absolute errors of 15.4%, 12.9% and 17.0%).

Conclusion The results demonstrate the potential for using in situ submersible spectrophotometer sensors to trace suspended sediment sources at high temporal frequency.

Keywords Sediment fingerprinting · UV–VIS spectrophotometer · High temporal frequency · In situ measurements · Sediment source tracing · MixSIAR

1 Introduction

Suspended sediment (SS) plays an essential role in the hydrological, geomorphological and ecological functioning of aquatic ecosystems (Owens et al. 2005; Bilotta and Brazier 2008; Wohl et al. 2015; Vercruysse et al. 2017). Suspended sediment export is mainly driven by hydrometeorological variables (Vercruysse and Grabowski 2019) and factors such as hillslope erosion, sediment delivery to stream channels and stream channel bank or bed erosion (Fryirs 2012; Mukundan et al. 2012). However, excessive amounts of SS can degrade aquatic ecosystems by causing siltation, habitat deterioration or pollution, linked to the key role of SS in the transportation of contaminants and nutrients (e.g. House 2003; Kronvang et al. 2003; Carter et al.

Responsible editor: David Allen Lobb

✉ Niels F. Lake
niels.lake@list.lu

[1] Catchment and Eco-Hydrology Research Group (CAT), Environmental Research and Innovation Department (ERIN), Luxembourg Institute of Science and Technology (LIST), L-4422 Belvaux, Luxembourg

[2] Centre for Environmental Science, School of Geography and Environmental Science, University of Southampton, Highfield, Southampton, Hampshire SO17 1BJ, UK

[3] Sustainable Agriculture Sciences, Rothamsted Research, North Wyke, Devon EX20 2SB Okehampton, UK

2006; Affandi and Ishak 2019). Hence, the need to identify the sources of SS is increasingly recognised as a priority to support management strategies for stream ecology, geomorphology and water quality issues (Walling and Collins 2008; Mukundan et al. 2012; Collins et al. 2017) in alignment with environmental policies (e.g. European Commission 2000).

Sediment fingerprinting is one direct approach to estimating SS contributions from catchment sources. This approach compares properties of potential source materials with properties of SS, using distinct diagnostic signatures or so-called composite fingerprints comprising several constituent properties (e.g. Oldfield et al. 1979; Peart and Walling 1988, 1986; Walling and Woodward 1992). These properties are selected on the basis that they are clearly distinctive between individual sources, allowing for the un-mixing of SS to estimate source proportions.

Despite the fingerprinting approach being increasingly adopted globally (see reviews by Haddadchi et al. 2013; Owens et al. 2016; Collins et al. 2017, 2020; Guan et al. 2017; Tang et al. 2019), there remain some major limitations that continue to hamper its use as either a scientific or management tool. These limitations include the pre-selection of the most robust fingerprints for different environmental settings (Koiter et al. 2013; Collins et al. 2020) and methods for SS sampling (Haddadchi et al. 2013). Robust fingerprint properties must both differentiate between potential SS sources and behave conservatively during mobilisation and delivery to the river, stream or lake (Walling et al. 1993). Conservative behaviour is important because erosion and SS transport processes are particle size selective which, in turn, influences sediment properties and the reliability of the direct comparisons between source materials and target SS samples (e.g. Collins et al. 2017; Laceby et al. 2017). A major limitation associated with common SS sampling methods concerns the limited insights they provide on how sediment sources change over short (i.e. minutes) time intervals and during longer (e.g. seasons or years) periods (e.g. Navratil et al. 2012; Vercruysse et al. 2017; Collins et al. 2020). The commonplace deployment of time-integrating samplers (Phillips et al. 2000), for example, is limited with regard to the temporal resolution of the SS source estimates generated (often limited to one or a small number of samples per event; Collins and Walling 2004). Furthermore, sediment particle size and geochemical properties might be altered during sampling deployment and sample storage prior to analysis (e.g. due to adsorption/desorption; Smith and Owens 2014). The collection and use of high frequency instantaneous SS samples are constrained by the associated analytical costs for many fingerprint properties/tracers commonly used in source fingerprinting investigations (Collins and Walling 2004; Haddadchi et al. 2013). High frequency observations (minutes) for prolonged periods could contribute to the understanding of catchment sediment dynamics (e.g. which SS sources are active under what conditions), which is key to eventually taking suitable countermeasures against excessive sediment input to rivers and streams (Navratil et al. 2012; Vercruysse et al. 2017).

The current absence of well-established methods to measure SS properties in situ at high frequency compounds the current limited capacity to document SS source contributions over short time intervals for longer durations of measurement. Thus far, attempts to overcome this limitation still rely on the collection of physical samples in the field at high frequency, in conjunction with subsequent laboratory analyses of tracer properties. Such work has included the use of diffuse reflectance infrared Fourier transform spectrometry (e.g. Poulenard et al. 2012; Cooper et al. 2015, 2014), spectral reflectance analysis of sediment chemical properties on samples placed on glass fibre filters (Martínez-Carreras et al. 2010a; Cooper et al. 2014), colour parameters obtained from spectro-colorimetry (Martínez-Carreras et al. 2010b), colour parameters derived from office scanners (Pulley and Rowntree 2016) and deployment of handheld XRF instruments (Smith and Blake 2014). Whilst these procedures reduce resource needs for the analysis of tracer properties in numerous target sediment samples, they do not overcome the resource needs pertaining to high frequency collection of such samples.

Submersible spectrophotometer sensors, widely used for drinking water quality monitoring (e.g. D'Acunha and Johnson 2019; González-Morales et al. 2020; Prairie et al. 2020), may, however, offer a reliable means to provide data on SS fingerprint properties at high frequency. Bass et al. (2011) and Martínez-Carreras et al. (2016) used submersible spectrophotometer sensors, measuring absorbance in the ultraviolet visible (UV–VIS) range, to estimate SS properties in situ. The former used such a sensor to estimate particulate organic carbon content, whilst the latter estimated sediment loss-on-ignition, with both studies calibrating the sensor readings using physical samples. This work demonstrated the potential value of such sensors to discriminate between sediment sources with contrasting tracer properties and for un-mixing source proportions. The ability of these sensors to measure in situ suggests limited physical SS sampling is only required for sensor validation. Furthermore, given the facility to measure at high frequency (e.g. minutes) for long duration, since maintenance needs of the sensor are low, a spectrophotometer sensor has the potential to resolve current constraints pertaining to both sediment sampling and ensuing tracer analysis.

When the influence of dissolved species in water is negligible, absorbance measurements are mainly affected by SS concentration (Thomas et al. 2017) and the size of the SS particles (Berho et al. 2004). Thomas et al. (2017) reported that absorbance increases with SS concentrations. Berho et al. (2004) showed that smaller particles resulted in higher absorbance values than coarser

particles with the same minerology. These studies clearly demonstrated that the exact relationships between absorbance and both concentration and particle size warrant detailed investigation to determine if, and to what extent, absorbance values need to be compensated to facilitate high frequency sediment source fingerprinting.

Given the above context and the ongoing need to continue testing devices for assembling high temporal resolution data on SS properties in situ, we conjecture that the absorbance readings of a submerged spectrophotometer can be used as sediment fingerprints to estimate SS sources. Herein, we present a proof-of-concept laboratory experiment where we use absorbance data to un-mix artificial mixtures of soil samples sieved to three different particle size fractions. To this end, we tested how the absorbance data is influenced by SS concentration and particle size distribution, as well as the suitability of the absorbance data for estimating sediment source proportions.

2 Materials and methods

Experimental assessment of the submersible spectrophotometer was undertaken in a series of laboratory tests. Soil samples of known origin and composition were used to create a series of water samples containing SS of differing composition and concentration; measurements of absorbance spectra in situ could then be interpreted in relation to the composition and concentration, and to the expected outcomes in terms of the spectra.

2.1 Soil samples and artificial mixtures

Six soil samples were collected in Luxembourg based on differences in colour (visual inspection) and differences in underlying geology (Fig. 1). Soils were air-dried at room temperature before being disaggregated manually using a pestle and mortar. Samples were then dry sieved to three different size fractions: < 32 µm, 32–63 µm and 63–125 µm. Due to its particle size distribution, retrieving the 63–125 µm fraction of soil 6 was not possible and this soil sample was therefore omitted, resulting in 17 size-fractionated soil samples. The fractions were selected based on commonly used upper particle size boundaries in sediment fingerprinting studies (see Laceby et al. 2017). Minerology of the soil samples is shown in Table A1.

From the resulting 17 size-fractionated soil samples, we created artificial mixtures of two, three and four different samples. Mixtures were classified into two groups: (i) mixtures of soil samples sieved to the same particle size fraction

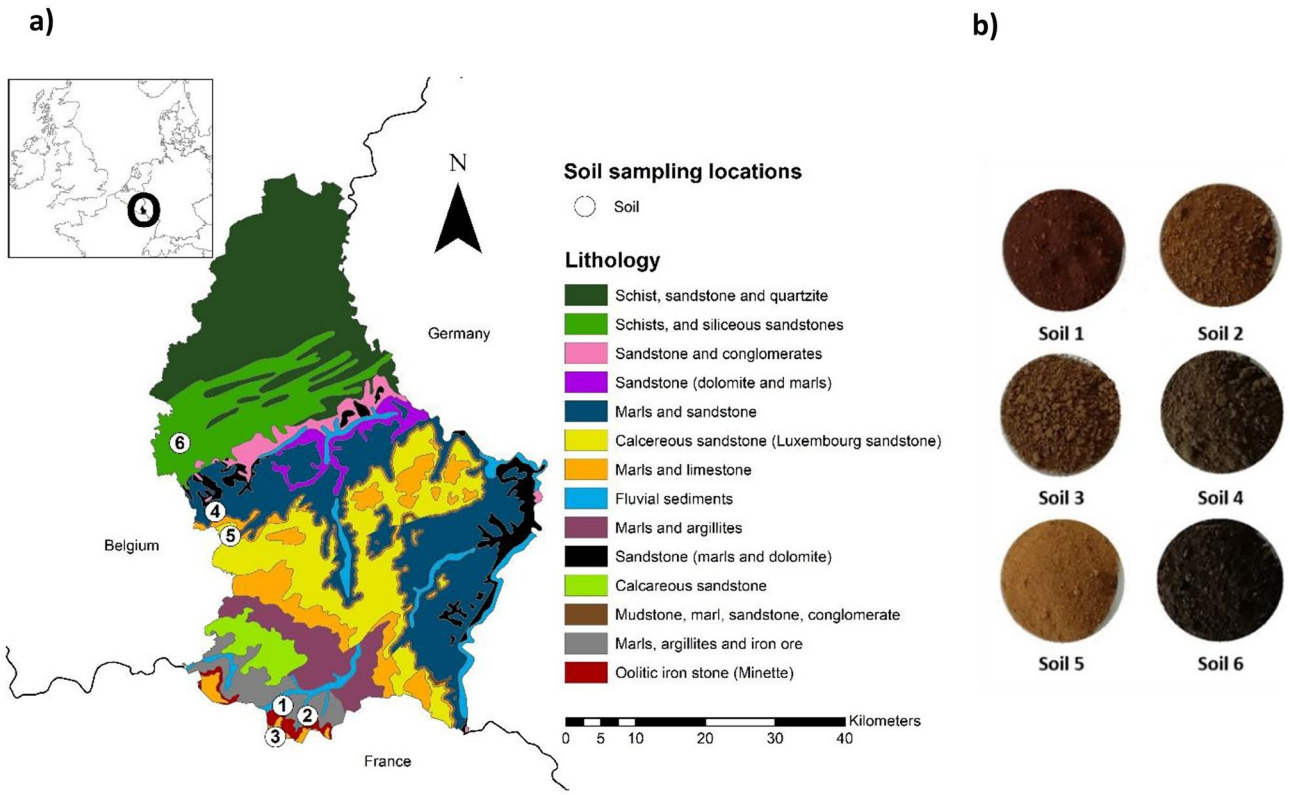

Fig. 1 Soil sampling locations within Luxembourg **a** and images of the six collected soils **b**. Source N.W. Europe map **a** adapted from: ArcGIS online (Europe_data_WG_NPS); source geological map of Luxembourg **a**: Service Géologique du Luxembourg

and (ii) mixtures of soil samples sieved to different size fractions. The soil sample contributions to the artificial mixtures were based on having either a clearly dominant sample or more equal contributions (see Table A2).

2.2 Sensors

Laboratory experiments used the S::can spectro::lyser™ probe (Scan Messtechnik GmbH, Vienna, Austria) submersible spectrophotometer. This sensor measures transmittance of a light beam (i.e. xenon-flash light) after contact with water in the optical measurement window, which is then converted to absorption over the UV–VIS wavelength range (200–730 nm, at 2.5-nm intervals). The detector is located at the opposite side of the optical window. Measurement frequency was set at 2-min intervals, which is the smallest interval possible. Measured absorbance data were saved onto the corresponding Con::cube logger (Scan Messtechnik GmbH, Vienna, Austria).

In tandem with the spectrophotometer, a LISST-200X laser diffraction (Agrawal and Pottsmith 2000) sensor (Sequoia Scientific, Bellevue, WA, USA) was used to measure particle size distribution. This instrument works on the principle of laser diffraction with a laser beam emitted by a laser diode (Agrawal and Pottsmith 2000). The LISST sensor assigns the diffracted laser beams into one of 36 sediment size classes, providing estimates of particle size distribution and average particle size. Measurements were taken at 1.5-s intervals using the random shape model algorithm (Sequoia Scientific 2018).

2.3 Laboratory setup

The laboratory setup consisted of a 75.4-L capacity, round tank. The spectrophotometer and LISST sensor were installed in a horizontal orientation to prevent sedimentation of particles on the measuring windows (Fig. 2a, c). Using 40 L of demineralised water, both sensors were located more than 10 cm below the water surface as advised by the manufacturers.

Homogeneous concentrations inside the tank were established using a Fundamix vibromixer (DrM, Dr. Mueller AG, Switzerland), a vibrating device. This method avoids cone and vortex formation which are possible with rotational stirring techniques (Orlewski et al. 2018). To test homogeneity of concentrations during the experiments, water samples were collected at three locations within the tank setup (Fig. 2c) using a pipette (see Fig. A1, A2 and A3 for initial testing on vibromixer speed and position, and homogeneity of concentrations at different depth and locations; supplementary material). These samples were subsequently transferred into pre-weighted aluminium buckets, dried and weighed again to determine concentrations. These concentrations (hereafter referred to as 'measured concentrations') were determined for all theoretical concentrations (10 concentrations in total; 100–1000 mg L^{-1} at 100 mg L^{-1} increments) for all experiments (20 values associated with erroneous measurements were omitted). Selected theoretical concentrations are representative of SS concentrations values measured across Luxembourgish rivers (Martínez-Carreras 2010). The experiments consisted of testing the 17 soil samples individually, followed by testing the 25 artificial soil sample mixtures (see Table A2 for a detailed overview of the experiments and known soil sample contributions in the artificial mixtures and Protocol A1 for more detail of the steps adopted during the experiments and specific equipment settings).

2.4 Data pre-treatment

LISST background measurements, taken before each experiment, were saved onto the instrument and automatically compensated for by the LISST software during subsequent measurements. Accordingly, the spectrophotometer absorbance data were compensated by using the data collected before the start of the actual experiment (i.e. subtracting the background readings from all consecutive absorbance data readings acquired during each experiment). Data obtained from the spectrophotometer and LISST sensors were thus only affected by the soil sample materials added to the experimental tank, and not influenced by the properties of the demineralised water. Absorbance data were measured over a 10-min period at 2-min intervals; only the last four measurements were used for analysis (allowing time for the soil sample material to become fully mixed). LISST data were measured over the same 10-min period, with only the last 6 min of measurements used in subsequent analyses.

2.5 Concentrations and their relationship with absorbance

Both theoretical and measured concentrations do not fully represent the actual concentrations inside the experimental tank. The former is subject to the settling of particles during mixing, whereas the latter is subject to uncertainties associated with pipette sampling and the weighing of aluminium cups. Three steps were used to quantify to what extent measured concentrations (see Sect. 2.3) deviated from theoretical concentrations, and if deviations differed for the three particle size fractions investigated (i.e. < 32 µm, 32–63 µm and 63–125 µm). Firstly, differences between measured and theoretical concentrations were calculated

for the experiments using only soil samples. Measured concentrations were expressed as a percentage of theoretical concentrations, to assess whether there is a consistency in soil sample material losses. Secondly, 'expected' mixture concentrations were then calculated using a mass-balance (Eq. 1), using the measured concentrations of the soil samples and their known contributions to the artificial mixture. This value was then compared with the directly measured concentration of the mixture itself.

$$\text{Expected mixture concentration} = \sum_{j=1}^{n} \mathrm{w}_j \times conc_j \quad (1)$$

where w_j is the relative contribution of each soil sample to the artificial mixture ($j = 1$ to n, with n being the number of soil samples mixed), and $conc_j$ is the measured concentration for soil sample j (resulting from the individual soil sample experiments).

As a final step, we investigated the relationship of absorbance with both concentration and sieved particle size. To analyse patterns in the absorbance spectra for the 17 soil samples, the responses to increasing concentrations and particle size were examined. Randomly selected absorbance values were used at low, medium and high range spectra (210 nm, 400 nm and 700 nm, respectively, example shown in Fig. A4; supplementary material). Besides these three randomly selected absorbance values, the average absorbance value over the whole range of measured wavelengths (200–730 nm) was used. These values were scaled, dividing the absorbance values by their respective theoretical concentrations, to obtain average increases in absorbance per mg L^{-1} ($n = 10$, for the 10 concentrations) for each soil sample, with accompanying standard deviations. This process was designed to obtain more insight into how absorbance changes with concentration at the different selected wavelengths for all soil samples. These scaled absorbance values were then related to the particle size measured at every concentration in every experiment. Using the Mann–Whitney test, we tested if the absorbance values ($n = 10$, for the 10 concentrations) from the 17 soil samples were significantly different ($p < 0.05$). This test was carried out for the average absorbance values, as well as for the absorbance values resulting from the three selected wavelengths (210 nm, 400 nm and 700 nm). Absorbance data in this analysis were compensated for theoretical concentrations (see Sect. 3.1).

2.6 Linear additivity

The directly measured absorbance values from the artificial mixtures were compared with the absorbance values resulting from the individual soil sample experiments to test if (i) absorbance behaves as a linearly additivity property and (ii) the combination of relative absorbance values of the individual soil samples, as used in the artificial mixtures, results in similar absorbance values when directly measured on the mixture (Eq. 2).

$$\text{Expected mixture absorbance} = \sum_{j=1}^{n} \mathrm{w}_j \times Abs_j \quad (2)$$

where w_j is the relative contribution of each soil sample to the artificial mixture ($j = 1$ to n), and Abs_j represents the absorbance value of that particular soil sample j when measured individually. The absorbance data over the whole wavelength range (200–730 nm) was used (example shown in Fig. A4). This comparison was undertaken for all 10 different concentrations, for each mixture experiment, and compared with the measured mixture absorbance data corresponding to the same theoretical concentrations.

2.7 Un-mixing the artificial mixtures using the MixSIAR model

The MixSIAR Bayesian un-mixing model (Stock and Semmens 2016; Stock et al. 2018) open-source R package was used to un-mix the artificial mixtures, and investigate how a well-established model for sediment fingerprinting (e.g. Upadhayay et al. 2020; Wynants et al. 2020) deals with the highly collinear absorbance data. As model input, data obtained from the mixture experiments (mixture data) were used, together with the absorbance data from the single soil samples (i.e. soil source data). To investigate performances between concentrations, only sources and mixture absorbance data from the same theoretical concentrations were used. Source data were represented by the mean, variance and sample size (Blake et al. 2018). The MixSIAR model calculates the relative average contributions of each sample mixed and the corresponding standard deviations. For all model runs, the Markov chain Monte Carlo parameters were used according to the predefined 'short' settings (chain length = 50,000, burn = 25,000, thin = 25, chains = 3). Model convergence was evaluated using the Gelman-Rubin diagnostics (variables < 1.1). All models were run using the High Performance Computing facility at the Luxembourg Institute of Science and Technology. For the MixSIAR runs, the whole range of absorbance values was used, with each wavelength being regarded as a tracer. This resulted in 213 tracer values (wavelength range 200–730 nm, with 2.5-nm intervals). The known source contributions to each artificial mixture were compared with the source contributions estimated by the model. This comparison was made by calculating the absolute error (AE); the absolute difference between the known soil source contributions and the predicted source contributions was generated by MixSIAR.

3 Results

3.1 Concentrations and relationship with absorbance

The measured concentrations inside the tank were generally lower than the theoretical concentrations intended (Fig. 3); measured concentration decreased with increasing particle size. The relationship between measured and theoretical concentrations varied little at increasing concentrations for all soil samples in the < 32-µm fraction (Fig. 3). Measured concentrations represented ~ 90% of the theoretical concentrations. Corresponding standard deviations ranged up to 4% (for 95% of all measured concentration values), with the remaining 5% of the values having higher deviations (observed at lower theoretical concentrations; i.e. 100–300 mg L^{-1}).

For the two coarser fractions, measured concentrations showed larger deviations from the theoretical concentrations (Fig. 3). For the 32–63-µm fraction, average measured concentrations mostly ranged between 60 and 90% of the theoretical concentrations. The average measured concentrations for the 63–125-µm fraction mostly ranged from 30 to 75%, with soil 5 giving very low measured concentrations compared with the other soil samples. Despite the larger differences, the relationship between measured and theoretical concentrations remained constant with increasing concentrations for the separate soil samples (Fig. 3). These average values had low standard deviations (i.e. < 10% for 97.5% of the values and < 5% for 81% of the values for the 32–63-µm fraction; < 10% for 95% of the values and < 5% for 56% of the values for the 63–125-µm fraction).

Deviations between expected and measured mixture concentrations (Eq. 1) are shown in Table 1. Around 50% of the expected mixture concentrations showed a deviation of < 5% compared with the measured mixture concentrations. Around two-thirds of mixtures showed a deviation < 10%, and around 90% a deviation < 20%. Furthermore, deviations between expected and measured mixture concentrations decreased slightly when the number of soil samples in the artificial mixtures was increased.

Both when using theoretical (Fig. A5) and measured (Fig. A6) concentrations, strong correlations with absorbance measured at the three selected wavelengths (i.e. 210, 400, 700 nm) were observed, as well as for the average absorbance over all wavelengths. Using theoretical concentrations (Fig. A5), r^2 values were > 0.99, with the exception of soil sample #5.3 (soil 5, 63–125 µm fraction), where the r^2 values decreased to ~ 0.96–0.97.

Taking into consideration the finding that absorbance showed a slightly stronger correlation with theoretical concentration, together with the data presented above, it was decided to compensate absorbance data using the theoretical concentrations in the following final results of this laboratory experiment. For reference, figures using similar analysis as shown in Sect. 3.2 and Sect. 3.3 using measured rather than theoretical concentration are available for consultation in the supplementary material. Since deviations between measured and theoretical concentrations are essentially constant for each tested soil sample (i.e. deviation percentages are independent of theoretical concentrations; see Fig. 3), the calculated 'expected' mixture concentrations and the measured mixture concentrations should correspond (Table 1). These results confirm that there is no need to compensate absorbance readings for concentration effects when comparing soil samples and mixtures that are using the same theoretical concentrations.

3.2 Patterns in absorbance spectra

Average increases in absorbance were found to be greater for smaller than for larger particle sizes (Fig. 4). Standard deviations for all soil samples were relatively small, with values mostly < 10% compared with their average values. The exceptions here were standard deviations of 11.8%, 12.7% and 14.3% for soil samples #1.3, #6.2 and #5.3, respectively (Fig. 4a). Furthermore, soil sample #1.3 showed a deviation exceeding 10% for the 210-nm (14.3%) and 400-nm (12.4%) wavelengths (Fig. 4b, c). For the 700-nm wavelength (Fig. 4d), only soil sample #5.3 showed a deviation exceeding 10% (10.3%).

The Mann–Whitney test results (Table 2) showed that three pairs of soil samples were not significantly different (average of all wavelengths). Six pairs of samples were not significantly different for the 210-nm wavelength, and two pairs of samples were not significantly different for the 400-nm and 700-nm wavelengths, respectively. These pairs of

Table 1 Deviations between expected and measured artificial mixture concentrations

	Total *n* values	*n* values < 5% deviation (in %)	*n* values < 10% deviation (in %)	*n* values < 20% deviation (in %)
2-sample mixture	115	50 (43.5%)	71 (61.7%)	100 (87.0%)
3-sample mixture	65	30 (46.2%)	43 (66.1%)	60 (92.3%)
4-sample mixture	50	29 (58.0%)	35 (70.0%)	45 (90.0%)
All mixtures	230	108 (47.0%)	147 (63.9%)	201 (87.4%)

Table 2 Mann–Whitney test results for soil samples that were not significantly different ($p > 0.05$) for the average of all wavelengths, 210 nm, 400 nm and 700 nm. Soil samples are indicated by #soil. fraction, with 'soil' representing the test soils ($n = 6$, Fig. 1), and 'fraction' the sieved fraction size (.1 for < 32 µm; .2 for 32–63 µm; .3 for 63–125 µm)

Average of all wavelengths	*p*-value	210 nm	*p*-value	400 nm	*p*-value	700 nm	*p*-value
#1.3 and #3.3	0.58	#2.1 and #4.1	0.97	#1.3 and #3.3	0.48	#1.3 and #3.3	0.97
#1.3 and #5.2	0.19	#3.1 and #5.1	0.44	#3.3 and #5.2	0.85	#3.3 and #5.2	0.25
#3.3 and #5.2	0.44	#1.2 and #4.2	0.052				
		#1.3 and #3.3	0.12				
		#1.3 and #4.3	0.74				
		#2.3 and #3.2	0.089				

soil samples (Table 2) were also not significantly different when analysing the average of all wavelengths. From the pairs shown in Table 2, only 1 combination (#3.1–#5.1) was used together in an artificial mixture (Table A2).

Finer particle sizes (i.e. a smaller mean effective particle size measured with the LISST 200X sensor) resulted in larger average increases in absorbance per mg L^{-1}, whilst coarser particle sizes showed smaller average increases per mg L^{-1}. This relationship appears to be logarithmic, with an r^2 value of 0.78 (Fig. 5). Analyses performed when using measured concentrations, instead of theoretical concentrations, showed rather similar outcomes (Fig. A7 and Fig. A8).

3.3 Linear additivity

Comparison of expected and measured mixture absorbance (Eq. 2) generated deviations of generally < 20% (Fig. 6). This was true for all mixtures except for three values where the deviations were slightly higher. Furthermore, a high percentage of the values (57%, 63% and 82% for the two-, three- and four-soil sample mixtures, respectively) showed deviations of < 10%. Deviations of < 5% were noted for 35% (two-sample mixture), 25% (three-sample mixture) and 6% (four-sample mixture) of the artificial mixture values. Values can be positive or negative, indicating whether the expected absorbance (Formula 2) is higher or lower than the absorbance measured directly for the artificial mixture. In Fig. A9, the deviations between the expected and measured absorbance are shown, with absorbance being compensated for measured concentrations.

3.4 Un-mixing artificial mixtures (MixSIAR)

The MixSIAR calculations using the two-soil sample mixtures showed that dominant soil sample contributions were reliably predicted (Fig. 7, Fig. A10). MixSIAR predicted the correct dominant soil samples for ten out of eleven such mixtures. From these mixtures, eight showed an overestimation of the dominant soil sample. For mixture 11, the dominant sample was not well predicted, with MixSIAR outputting equal contributions of the soil samples mixed. For the one mixture using equal (50%)

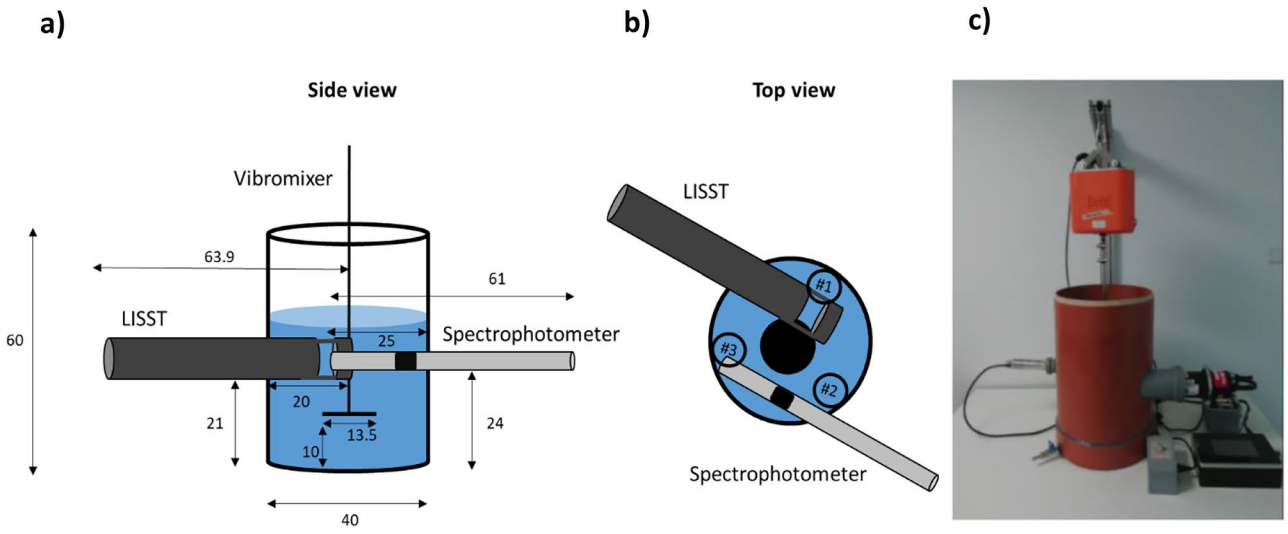

Fig. 2 Laboratory setup: **a** side view schematic representation with dimensions in cm; **b** top view schematic representation with water sampling locations #1, #2 and #3, and **c** photograph

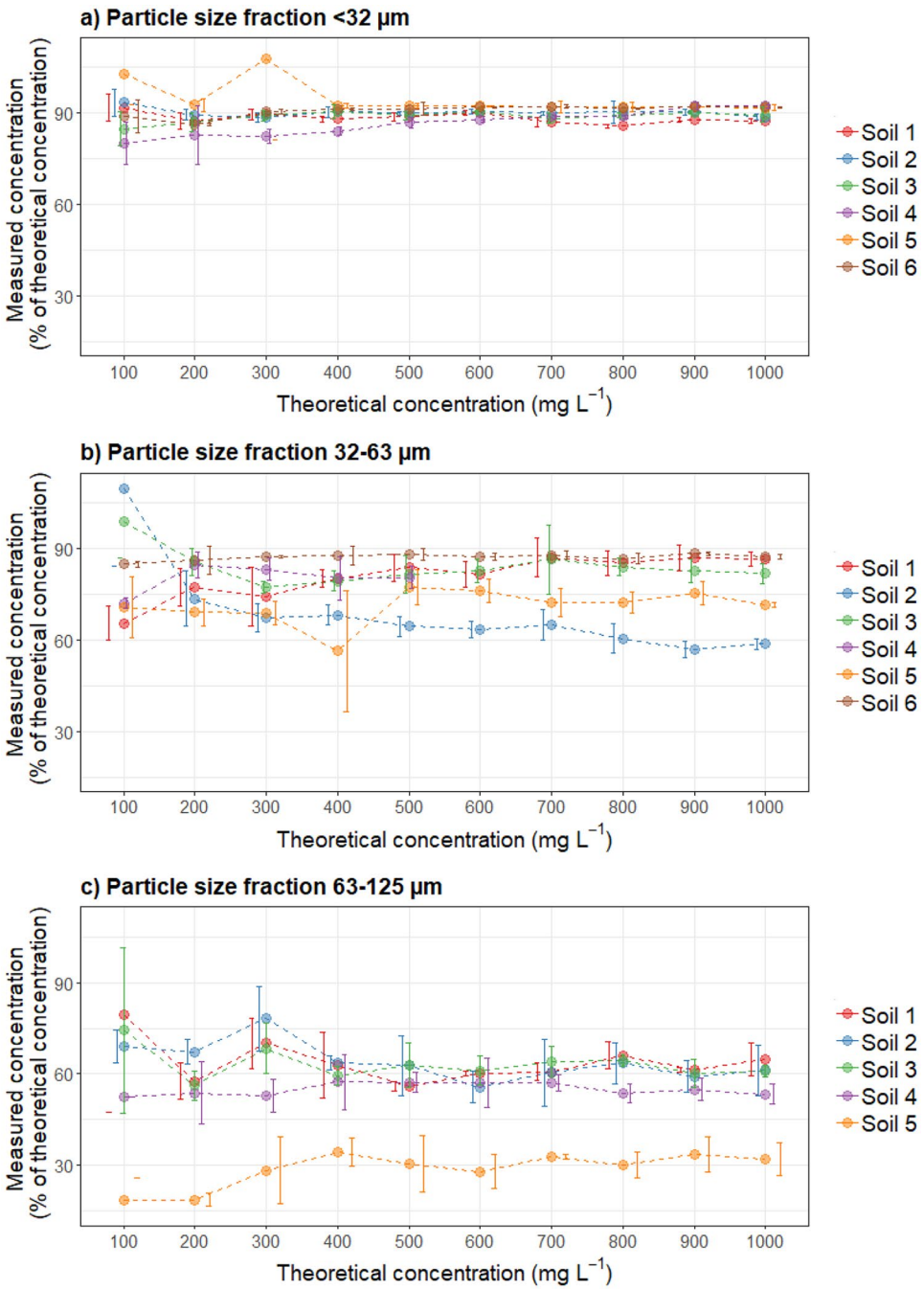

Fig. 3 Average and standard deviation ($n = 3$) of measured concentrations inside the experimental tank expressed as a percentage of the theoretical concentrations for the six test soils (Fig. 1), sieved to **a** < 32 µm, **b** 32–63 µm and **c** 63–125 µm. Error bars are plotted adjacent to the dots which represent the mean values

contributions (mixture 8), MixSIAR over-predicted (70%) and under-predicted (30%) the known relative contributions. The results of the tests using artificial mixtures with different particle size fractions (mixtures 10, 11 and 12) indicated there were no clear differences in MixSIAR predictions compared with those from the artificial mixtures using samples sieved to the same particle size fraction.

For the eight artificial mixtures using three soil samples, MixSIAR predicted the dominant soil sample contribution well in six cases. From these six cases, MixSIAR over-predicted the contribution of the dominant soil for mixtures 18 and 20, whereas it under-predicted the contribution of the dominant contributing soil sample for mixtures 14, 15, 16 and 17. Mixtures 18 and 20 were, together with mixture 17, the mixtures using samples sieved to different particle size fractions. In the case of mixture 19, MixSIAR predictions deviated from the known inputs, with the more dominant soil sample (50%) constantly being predicted by the model as the soil sample with least contribution.

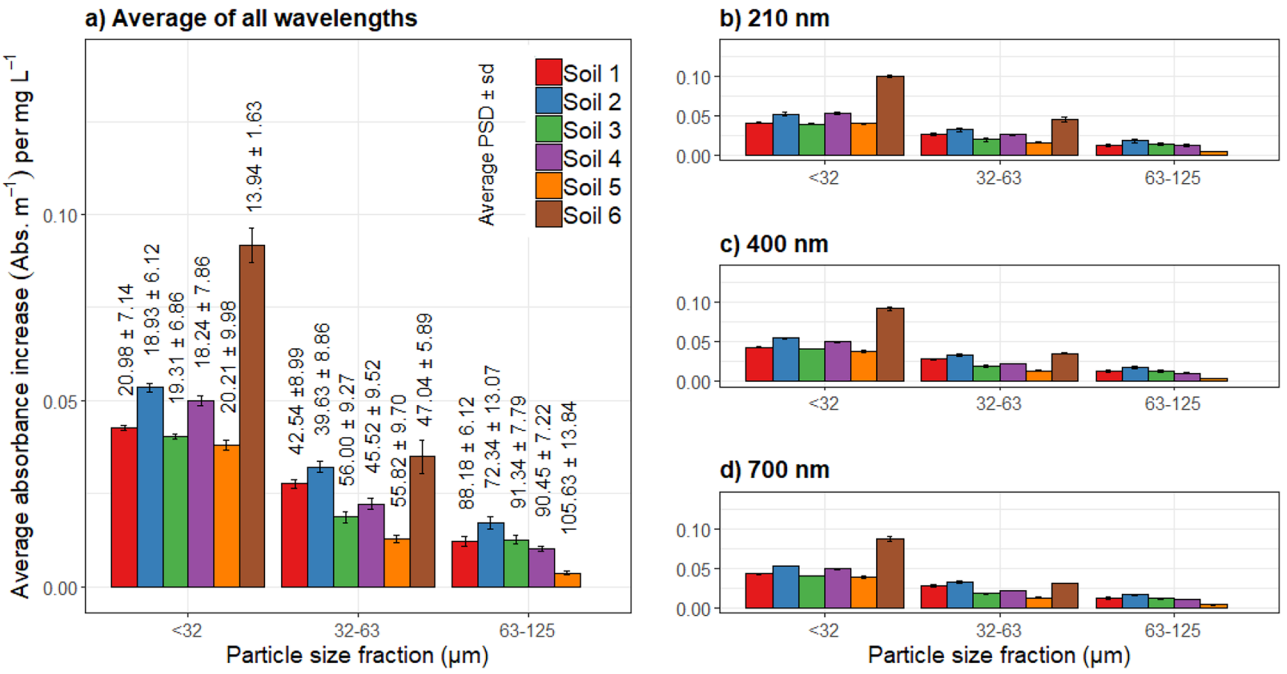

Fig. 4 Average increases in absorbance per mg L^{-1} (absorbance values divided by theoretical concentrations) for average absorbance over **a** all wavelengths, **b** 210 nm, **c** 400 nm and **d** 700 nm, for all 17 soil samples (indicated by #soil.fraction, with 'soil' representing the test soils ($n=6$), and 'fraction' the sieved fraction size (.1 for < 32 µm; .2 for 32–63 µm; .3 for 63–125 µm). Values inside the plot refer to the average (PSD) and standard deviation (SD) of measured particle size distributions per sample and dry sieved fraction measured with the LISST sensor inside the experimental tank

For the four-soil sample mixtures, four out of five were mixed to have a clearly dominant contributing (70%) soil sample. Dominant contributions in mixtures 21 (under-estimated compared to known input) and 25 (over-estimated compared to known input) were predicted by MixSIAR. For mixture 22, the model failed to predict a dominant soil sample, and for mixture 24, an erroneous soil sample was predicted as the dominant source. In the case of mixture

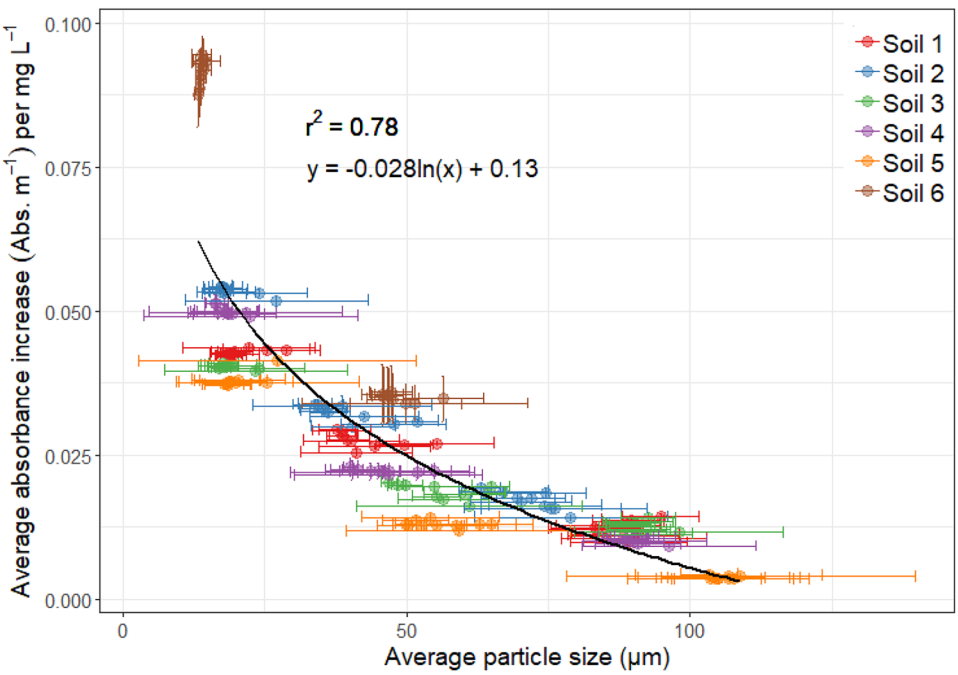

Fig. 5 Relationship between average increases in absorbance per mg L^{-1} (absorbance values divided by theoretical concentrations) as a function of average particle size measured with the LISST sensor inside the experimental tank. Particle size values and corresponding standard deviations were calculated for every sample and for every concentration separately

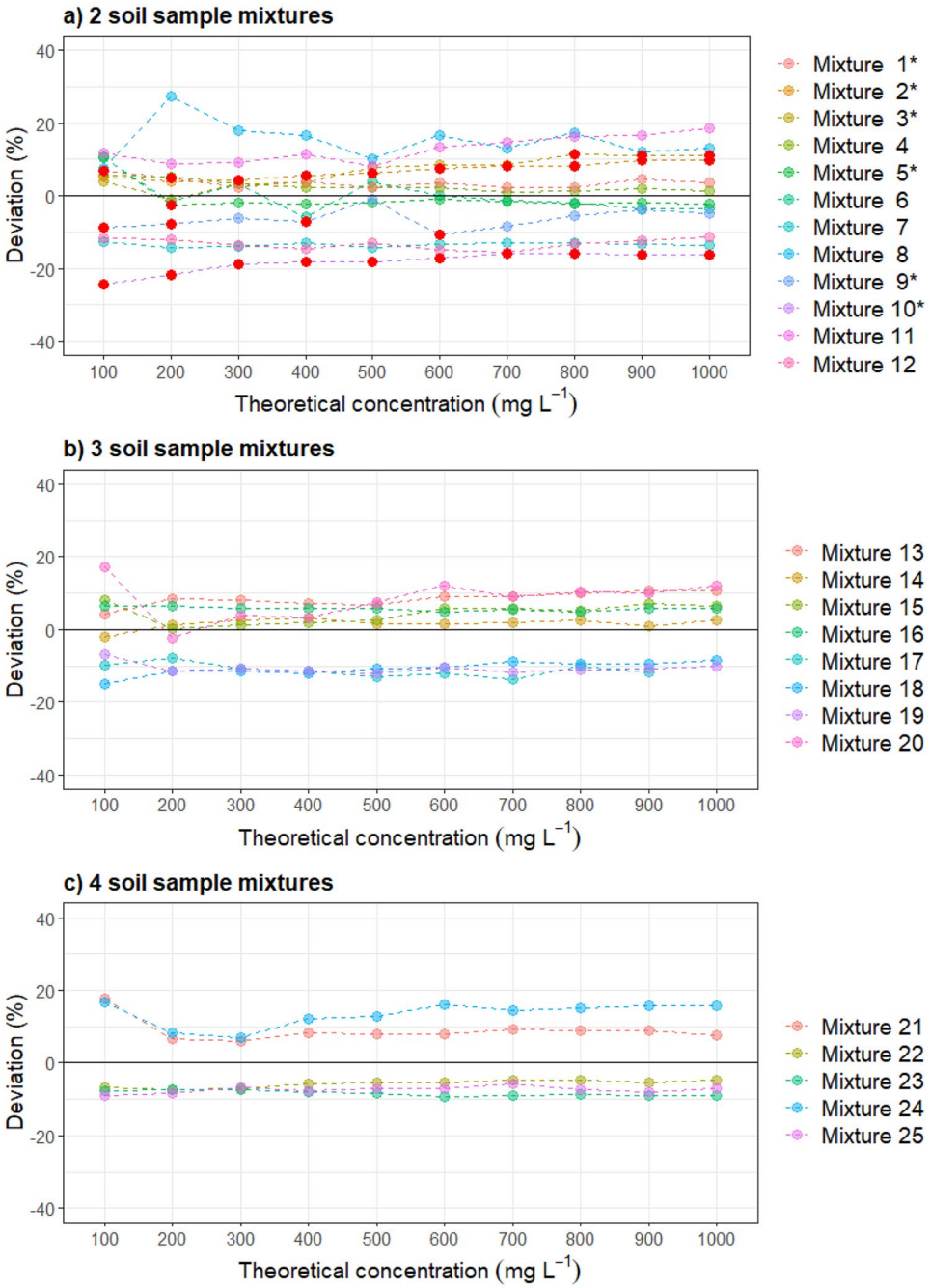

Fig. 6 Deviations between measured absorbance and 'expected' absorbance based on a single soil sample absorbance signal (mass-balance), shown for **a** two-, **b** three- and **c** four-soil sample mixtures. Red dots **a** indicate those situations in which absorbance values from the artificial mixtures are larger or smaller than the absorbance values measured for both individual soil samples comprising that mixture (concerned mixtures are indicated by * in the legend)

23, with known equal (25%) proportions for all four soil samples, the predictions from MixSIAR showed variable levels of agreement.

Table A3 presents an overview of the accuracy of the MixSIAR predictions relative to the known soil sample proportions comprising the different artificial mixtures. Absolute errors varied between 6 and 26.7% for the two-sample mixtures, between 1.8 and 41.0% for the three-sample mixtures, and between 2.8 and 48.8% for the four-sample mixtures. Standard errors for the MixSIAR predictions were also calculated, returning values ranging up to 6.2%, 10.7% and 3.2% for the two-, three- and four-soil sample mixtures, respectively. Not all models passed the Gelman-Rubin diagnostics, where variables exceeding the value of 1.1 were observed in one or several concentrations within five out of eight three-sample mixtures and in all five four-sample mixtures. Details on the Gelman-Rubin diagnostics are shown in Table A4.

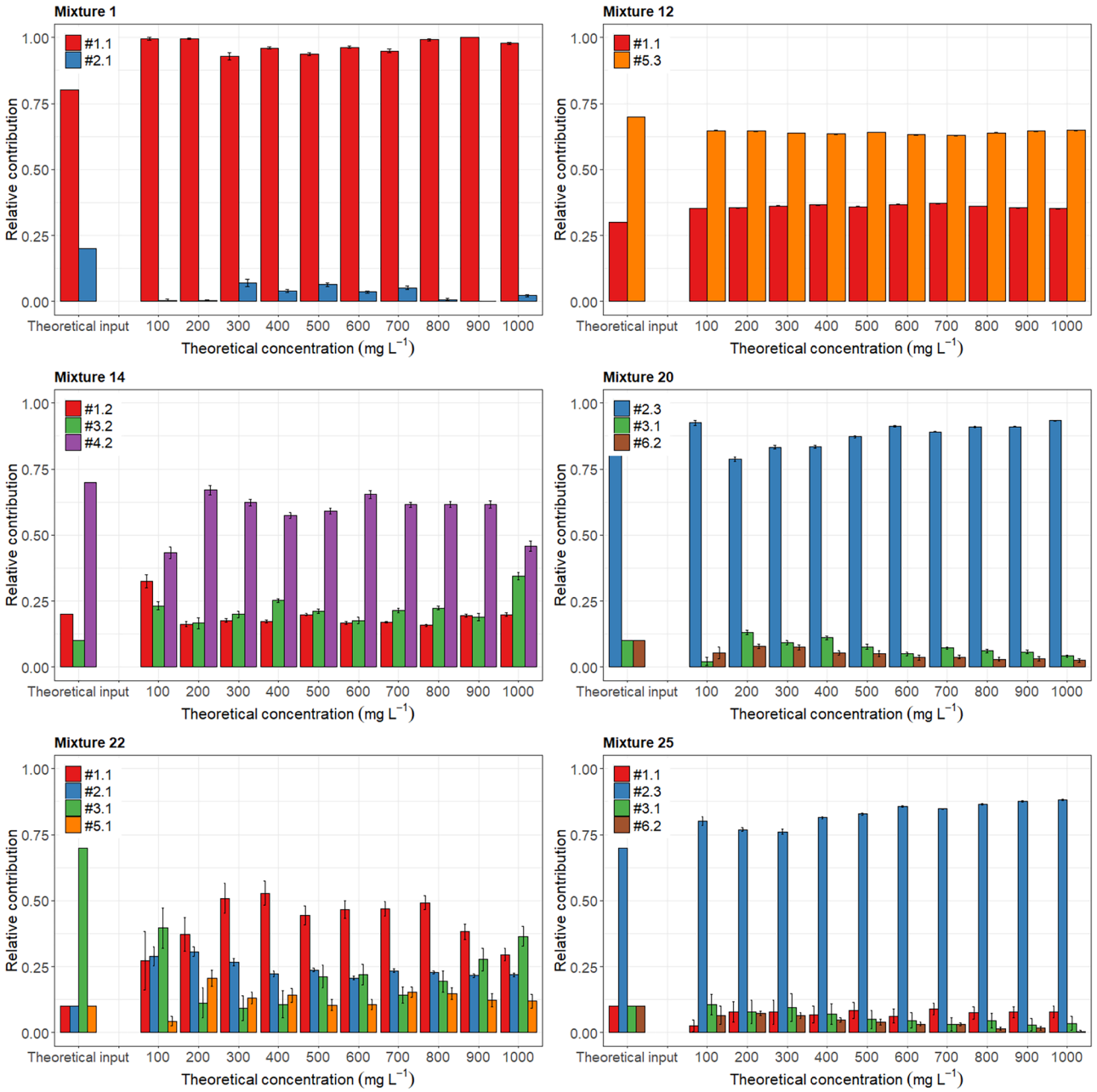

Fig. 7 Selection of un-mixing results for artificial mixtures of two soil samples (mixtures 1 and 12), three soil samples (mixtures 14 and 20) and four soil samples (mixtures 22 and 25) using MixSIAR at increasing theoretical concentrations. Model predictions are compared with the known proportions (theoretical input) of soil samples mixed (indicated by #soil.fraction, with 'soil' representing the test soils ($n = 6$), and 'fraction' the sieved fraction size (.1 for < 32 µm; .2 for 32–63 µm; .3 for 63–125 µm)

4 Discussion

4.1 Specific considerations for using the high frequency spectrophotometer approach

Absorbance data are known to be influenced by concentration (Thomas et al. 2017). Our results show that concentrations are strongly linearly correlated with absorbance (Fig. A4 and A5). However, the correlations are soil sample-dependent, which renders it necessary to correct the absorbance data from each soil sample with its specific concentration when comparing different soil samples. As the aim here was to un-mix artificial mixtures into the known individual contributions of the constituent samples, it is essential to make sure that compensation is made for the correct concentrations in order to avoid over- or under-estimations of

contributions. To this end, theoretical input concentrations were compared with measured concentrations. Theoretical concentrations are subject to the mixing processes inside the tank and the possible incomplete suspension of particles. This latter process seems to be important in the measured concentration results, showing that samples sieved at a larger mesh size deviate more from theoretical concentrations (Fig. 3). Despite this observation, and based on the data shown in Fig. 3 and Table 1, losses observed in measured concentrations were consistent. These concentrations were, however, subject to representative sampling and weighing errors, and show slightly weaker correlations with absorbance, hence the use of theoretical concentrations in this study.

In addition to the influence of concentration, particle size affects absorbance readings (Berho et al. 2004). Finer particles, at the same concentrations, resulted in higher absorbance values over the whole range of wavelengths compared with particles with coarser sizes. Together with the influence that particle size can have on sediment properties (Collins et al. 2017; Laceby et al. 2017), different particle sizes can also induce different absorbance patterns over specific wavelength ranges, as certain wavelengths might be subject to specific SS properties (Byrne et al. 2011). These differences were, however, found to be rather small in the present study (Figs. 4 and A7) when compared with the effects of concentration and particle size. Since the LISST sensor measurements showed that particle size is an intrinsic SS property remaining unchanged (assuming minimal dissolution of particles and minimal breakdown of particles in suspension) during the experiments presented here, the analysis focused more on the compensation of absorbance in relation to concentration so as to allow proper comparisons between the absorbance values of the soil sources and between the absorbance values of the soil sources and target SS.

Effective tracers or fingerprints should behave in a linearly additive manner (Walling et al. 1993; Lees 1997). Our results show that the absorbance readings of particles suspended in distilled water are linearly additive (Fig. 6) and consistently so over the range of concentrations tested. Some deviations were found, however, at the lower concentrations, which are likely to be due to the smaller amounts of particles and thus larger relative errors where mixing is inconsistent or incomplete. In testing the linear additivity, artificial mixtures containing samples sieved to the same or different particle size fractions were used. The two groups of samples did not show significantly different results for linear additivity (Fig. 6). Tests in which only finer or only coarser size fractions were used did not result in clear differences in the linear additivity.

The un-mixing results using the MixSIAR model followed a similar pattern to the results for the linear additivity tests. Higher deviations between modelled and known soil sample proportions occurred at the lowest concentrations but were found to deviate less at higher concentrations. No significant difference in performance was found when un-mixing soil samples sieved to the same or different particle size fractions (Table A3). These results contrast with observations reported by Gaspar et al. (2019), who found estimations were less reliable at finer particle sizes. Gaspar et al. (2019) tested the un-mixing performance of artificial soil mixtures (dry material), looking at geochemical composition, using estimations from the FingerPro model. However, these authors only sieved one mixture to three different size fractions (with 10 replicates for each fraction) whereas the source samples were sieved to just one fraction (< 63 µm). On the contrary, in the present study, the soil sources were sieved to different size fractions (no replicates, with different concentrations tested). Our approach thus results in a comparison between mixtures and sources with a common particle size range and helps to eliminate uncertainties in the un-mixing induced by particle size.

It is informative to compare results of the present study to others with respect to the accuracy of un-mixing, although it is important to acknowledge that un-mixing model structures vary and this can influence performance. Haddadchi et al. (2014) tested four different mixing models (Modified Hughes, Modified Collins, Landwehr and Distribution models) using the geochemical properties of sources and mixtures, with mixtures being artificially created. Maximum model deviations ranged from 10.8 to 29% depending on the model used, indicating that therefore the choice of the un-mixing model is an important consideration, with the choice partially depending on the type of tracer used (Haddadchi et al. 2014). Gaspar et al. (2019) reported a maximum AE of 10% for un-mixing using both dominant and non-dominant mixtures (using elemental geochemistry). The present study, in comparison, found AE > 10% in most of the 25 different mixtures (except 2 out of the 12 two-sample mixtures and 3 out of the 8 three-sample mixtures), with maximum AE up to 26.7% for two-sample mixtures, 41.0% for three-sample mixtures and 48.8% for four-sample mixtures. The observed high AE for the three-sample mixtures is an extreme value however, since the second highest AE shows a value of 27.7%. Furthermore, the extreme outlier in the three-sample mixtures was found in mixture 19 where soil sample contributions added were rather equal (20%, 30%, 50%), whilst the extremes in the four-sample mixtures were found in mixtures 22 and 24 where there was a clear dominant soil sample present (70%, with other soil sample contributions of 10%). These results suggest that the absorbance readings from a submerged spectrophotometer can be used as fingerprints and thus to estimate the soil sample contributions of two- and three-sample artificial mixtures with similar accuracy than the existent methods. However, some of the four-sample

artificial mixtures showed unacceptably high AE, showing the limitation of the method to distinguish four soil samples when these present similar absorbance signals.

Models for the three- and four-sample mixtures did not always converge, exceeding the Gelman-Rubin diagnostics threshold value. Tests showed that increasing the number of iterations (chain length) improved the diagnostics for certain mixtures. However, we decided not to extend beyond the selected 'short' settings due to long computation times (> 5 days for each model run). Furthermore, we observed that, for all but one mixture, certain concentrations satisfied the diagnostics. Combined with the consistency in modelling results over the different concentrations within each mixture, this indicated the reliability of the modelling outcomes for those situations in which the diagnostics were not satisfied.

These highest AE values found herein can be partly explained by examining the spectra in more detail. For the two source artificial mixtures, the high AE (20%) values were seen in situations where the mixture absorbance values did not fall in between the range of absorbance values of the individual soil samples mixed (i.e. the artificial mixture has lower or higher absorbance values compared to the values of the individual soil samples; see also red dots indicated in Fig. 6). Failures can be due to small deviations in concentrations (e.g. settling), as expected and aimed concentrations slightly differ (Fig. 3). Such situations violate the so-called bracket or range test used as a conventional screening step in sediment source fingerprinting decision trees (Collins et al. 2017). Failure of the bracket test was only observed in the case of mixtures using two soil samples (Fig. 6a; for 23% of the total values here). Using measured instead of theoretical concentrations did not improve this result, resulting in a larger number of violations (Fig. A9). In the three soil source mixtures, predicted soil source contributions seemed to vary between soil samples that show a similar course of absorbance values over the whole range of measured wavelengths. This was, for example, observed for mixtures 13 and 16. MixSIAR failed to predict one clear dominant soil sample in these mixtures (i.e. 70% and 80% dominant soil samples used as input), but rather predicted two soil samples each with relatively high contributions around 40–50%. These two soil samples exhibit the same absorbance patterns (i.e. the absolute differences between the absorbance values of the soil samples are highly similar at all wavelengths tested); using the model to predict the dominant soil sample under such circumstances is problematic. The same pattern holds for the four-soil sample mixtures; in both mixtures 22 and 24 (with the highest reported AE values), the model failed to predict the dominant soil source. Both these mixtures used soil samples 1.1 and 3.1, which had absorbance values that showed minimal deviations between them (absolute values) and followed the same patterns (i.e. small absolute differences between all wavelengths tested), making it difficult for the model to differentiate between these two soil source samples. Furthermore, the mixture absorbance data in both these mixtures plotted exactly in between the absorbance values of the two soil samples; this most likely caused the model to fail to predict the correct dominant soil source. This outcome can be observed in Fig. A10, where model predictions show more equal contributions for the artificially mixed soil samples (mixture 22) and a more dominant soil sample 1.1 (mixture 24) despite soil sample 3.3 being the dominant soil source in both mixtures.

Scaling up beyond the laboratory scale, it would be informative to use independent evidence to validate any source apportionment estimates using absorbance spectra (which need to be statistically significantly different for the individual sources in question). However, this requirement for independent evidence is difficult to fulfil meaning that many source fingerprinting studies continue to rely on the use of mixture tests as verification of predicted source proportions (Collins and Walling 2004).

4.2 Wider implications for SS fingerprinting

The use of sensors that measure spectrophotometrically at high frequency in situ substantially reduces the need for extensive analyses in the laboratory in conjunction with the collection of conventional physical water samples; such sensors thereby allow much faster acquisition of tracer data (Martínez-Carreras et al. 2016), due to the in situ measurements. Therefore, despite the initial purchasing costs of the spectrophotometer (~ 20,000 USD), and the need to control for sensor drifts to validate the absorbance data results (Gamerith et al. 2011), total costs decrease over time. This is in contrast to classical sediment fingerprinting approaches, wherein laboratory analyses of all samples are required (e.g. different geochemistry analyses estimated at as much as ~ 1500–2000 USD per sample; Horowitz 2013), increasing both labour and analysis costs substantially when increasing measurement intervals and sampling campaign duration. The collection of absorbance data in situ could therefore improve the temporal resolution of sediment source fingerprinting and eventually give better insights into how sources of SS change over short time scales. This evidence gap has been highlighted by Navratil et al. (2012) and Vercruysse et al. (2017), who argued that a better understanding of sediment dynamics over short time scales is key to improving sediment transport modelling and for devising more robust solutions to catchment sediment management problems. With regard to the present study, it clearly remains important to test the use of the spectrophotometer for un-mixing source contributions in real-world settings, including at catchment scales. In the experiments here, using Luxembourgish soil samples with differences in both colour and expected geochemistry, absorbance data of the soil samples were in most

situations sufficiently different for un-mixing. It is therefore a prerequisite to investigate if absorbance spectra responses of potential SS sources in a real-world setting are sufficiently different enough to allow source discrimination.

Initial steps to identify areas or sources that could permit robust discrimination could be based on, for instance, differences in underlying geology as was done in this study. Looking at the results presented herein, seeing the uncertainties associated with four-sample mixtures, applying this approach in a field setting might require the selection of a limited number of potential sources to avoid poor discrimination and thus poor source apportionment results. Another approach that could potentially increase the ability to differentiate between sediment sources could be achieved by selecting only a number of wavelengths (i.e. selecting those tracers that best discriminate between sources). Reducing the number of tracers could also overcome issues with the long model calculation times faced when using all wavelengths as tracers.

Dissolved compounds in natural waters (e.g. nitrates and DOC) will influence the absorbance readings of the spectrophotometer (D'Acunha and Johnson 2019). Furthermore, the composition of the water (which was compensated for in the present study by subtracting the blank water background signal from the absorbance data) may well fluctuate in field settings (Wilson et al. 2013). To establish this background signal in field conditions might be challenging and ways to overcome this remain to be investigated. One possible solution to this challenge might be to use only absorbance values from those wavelengths that are less responsive to dissolved compounds. This consideration warrants further research.

In our proof-of-concept laboratory experiments, the individual soil sample ('source') absorbance spectra were sufficiently able to un-mix the majority of the absorbance spectra of the artificial soil mixtures. However, the absorbance signatures of potential SS sources (e.g. surface soils and channel banks) would be difficult to obtain because the spectrophotometer employed in this study is only able to measure whilst submerged. One approach here could be to sample material being mobilised and routed from potential sources towards the river channel (e.g. from rill erosion, or during/immediately after rainfall events when clear patterns of erosion or mobilisation of source materials have emerged). Such intermediate sampling would help address uncertainties associated with particle size selectivity (Laceby et al. 2017) and ensure, when measuring in a laboratory experiment as presented in this study, direct comparison of absorbance spectra representative of eroded material from individual sources with the spectra for SS. Clearly, however, the use of the approach reported herein would face challenges for some source types on this basis, with the obvious problematic source being eroding channel banks. Given the juxtaposition of banks to the river water, all particle size fractions are delivered to the water column, since there is no runoff pathway to result in selective delivery. Given this issue, it is more likely that the use of spectrophotometers in situ will be more relevant to un-mixing spatial SS sources using a confluence-based approach (e.g. Wynants et al. 2020). Here, sensors could be placed near the outlets of tributaries to create an archive of absorbance spectra of tributary-based spatial sources and on the main stem further downstream to represent the spectra of target SS. Concentration issues could be handled similarly to the laboratory experiment reported herein since by dividing the absorbance of both sources (i.e. tributaries) and the main stem measurements by the measured concentrations (which could be estimated using sediment rating curves, showing the relationships between SSC and turbidity using either turbidity meters or using the turbidity measured by the spectrophotometer itself), they can be scaled to the same SS concentrations (Fig. 4). Spectrophotometers can be equipped with an automatic brush (ruck::sack; Scan Messtechnik GmbH, Vienna, Austria) that cleans the sensor lens before every measurement. Next to that, optical sensors require regular maintenance to avoid instrument drifts caused by biofouling (e.g. bi-weekly cleaning as proposed by Martínez-Carreras et al. 2016).

5 Conclusions

The following conclusions can be drawn from the laboratory experiments conducted herein:

(1) Absorbance data and concentration show a strong linear relationship. It is thus essential to compensate absorbance data with concentration to un-mix different sources in artificial mixtures.
(2) There is a logarithmic relationship between absorbance and particle size, with a strong influence of particle size on the absorbance data with increasing concentrations (e.g. finer particle sizes result in higher absorbance values per mg L^{-1}).
(3) Absorbance data behave in a linearly additive manner, with deviations between expected and measured absorbance for artificial mixtures being < 20% for all comparisons and < 10% for more than half of the cases.
(4) The MixSIAR model mostly successfully un-mixed the artificial soil sources (with an average AE of 14.9% for all soil samples in all mixtures), correctly predicting dominant soil samples in the mixtures. The MixSIAR model worked better for the two- and three-soil sample mixtures in the present study. Results for the four-sample mixtures were less promising, but most likely inherent to the choice of soil samples used in those mixtures.

To be able to use the approach described in field settings, the following issues must be addressed:

(1) There is a need to create robust methods to define sediment source absorbance signals. A key challenge here is the selection of the most appropriate sediment particle size to define source material absorbance. A prerequisite is that the sediment sources result in absorbance signals that are sufficiently different to provide a basis for robust source discrimination and apportionment.
(2) Concentrations of SS need to be measured accurately. This information is needed to compensate the absorbance data for concentration in order to compare source absorbance data with the corresponding target SS data.

Supplementary Information The online version contains supplementary material available at https://doi.org/10.1007/s11368-021-03107-6.

Acknowledgements We would like to thank François Barnich for his help constructing the tank setup and Christophe Hissler for his help in the selection of the soil sampling locations. We thank Dhruv Sehgal for the help on the tank setup design and discussions during various stages in the data analysis.

Author contribution NFL, NMC, ALC and PJS conceptualised the experiment. NFL and NMC designed the laboratory setup with the help of PJS and ALC. NFL and NMC collected the soil samples. NFL sieved the soil samples to different fractions and executed the experiments. NFL analysed the data under the supervision of NMC, PJS and ALC. NFL wrote the manuscript and all authors revised and edited. NMC acquired the financial support for the project. All authors approved the final version of the manuscript.

Funding This research was funded by the Luxembourg National Research Fund (FNR), (PAINLESS project, C17/SR/11699372). Rothamsted Research receives strategic funding from the UKRI-BBSRC (UK Research and Innovation – Biotechnology and Biological Sciences Research Council) and the contribution by ALC was funded by grant award BBS/E/C/000I0330.

Data availability Absorbance data for all soil sample and mixture experiments, as well as the measured concentrations in the tank setup during all experiments, are available at zenodo.org (Lake et al. 2021; https://doi.org/10.5281/zenodo.5713544). For more information please contact the authors (Niels Lake, niels.lake@list.lu; Núria Martínez-Carreras, nuria.martinez@list.lu).

Code availability Not applicable.

Declarations

Conflict of interest The authors declare no competing interests.

References

Affandi FA, Ishak MY (2019) Impacts of suspended sediment and metal pollution from mining activities on riverine fish population—a review. Environ Sci Pollut Res 26:16939–16951. https://doi.org/10.1007/s11356-019-05137-7

Agrawal YC, Pottsmith HC (2000) Instruments for particle size and settling velocity observations in sediment transport. Mar Geol 168:89–114. https://doi.org/10.1016/S0025-3227(00)00044-X

Bass AM, Bird MI, Liddell MJ, Nelson PN (2011) Fluvial dynamics of dissolved and particulate organic carbon during periodic discharge events in a steep tropical rainforest catchment. Limnol Oceanogr 56:2282–2292. https://doi.org/10.4319/lo.2011.56.6.2282

Berho C, Pouet MF, Bayle S, Azema N, Thomas O (2004) Study of UV-vis responses of mineral suspensions in water. Colloids Surfaces A Physicochem Eng Asp 248:9–16. https://doi.org/10.1016/j.colsurfa.2004.08.046

Bilotta GS, Brazier RE (2008) Understanding the influence of suspended solids on water quality and aquatic biota. Water Res 42:2849–2861. https://doi.org/10.1016/J.WATRES.2008.03.018

Blake WH, Boeckx P, Stock BC, Smith HG, Bodé S, Upadhayay HR, Gaspar L, Goddard R, Lennard AT, Lizaga I, Lobb DA, Owens PN, Petticrew EL, Kuzyk ZZA, Gari BD, Munishi L, Mtei K, Nebiyu A, Mabit L, Navas A, Semmens BX (2018) A deconvolutional Bayesian mixing model approach for river basin sediment source apportionment. Sci Rep 8:1–12. https://doi.org/10.1038/s41598-018-30905-9

Byrne AJ, Chow C, Trolio R, Lethorn A, Lucas J, Korshin GV (2011) Development and validation of online surrogate parameters for water quality monitoring at a conventional water treatment plant using a UV absorbance spectrolyser. Proc 2011 7th Int Conf Intell Sensors. Sens Networks Inf Process ISSNIP 2011:200–204. https://doi.org/10.1109/ISSNIP.2011.6146515

Carter J, Walling DE, Owens PN, Leeks GJL (2006) Spatial and temporal variability in the concentration and speciation of metals in suspended sediment transported by the River Aire, Yorkshire, UK. Hydrol Process 20:3007–3027. https://doi.org/10.1002/hyp.6156

Collins AL, Blackwell M, Boeckx P, Chivers CA, Emelko M, Evrard O, Foster I, Gellis A, Gholami H, Granger S, Harris P, Horowitz AJ, Laceby JP, Martinez-Carreras N, Minella J, Mol L, Nosrati K, Pulley S, Silins U, da Silva YJ, Stone M, Tiecher T, Upadhayay HR, Zhang Y (2020) Sediment source fingerprinting: benchmarking recent outputs, remaining challenges and emerging themes. J Soils Sediments 20:4160–4193. https://doi.org/10.1007/s11368-020-02755-4

Collins AL, Pulley S, Foster IDL, Gellis A, Porto P, Horowitz AJ (2017) Sediment source fingerprinting as an aid to catchment management: A review of the current state of knowledge and a methodological decision-tree for end-users. J Environ Manage 194:86–108. https://doi.org/10.1016/j.jenvman.2016.09.075

Collins AL, Walling DE (2004) Documenting catchment suspended sediment sources: problems, approaches and prospects. Prog Phys Geogr Earth Environ 28:159–196. https://doi.org/10.1191/0309133304pp409ra

Cooper RJ, Krueger T, Hiscock KM, Rawlins BG (2015) High-temporal resolution fluvial sediment source fingerprinting with uncertainty: A Bayesian approach. Earth Surf Process Landforms 40:78–92. https://doi.org/10.1002/esp.3621

Cooper RJ, Rawlins BG, Lézé B, Krueger T, Hiscock KM (2014) Combining two filter paper-based analytical methods to monitor temporal variations in the geochemical properties of fluvial suspended particulate matter. Hydrol Process 28:4042–4056. https://doi.org/10.1002/hyp.9945

D'Acunha B, Johnson MS (2019) Water quality and greenhouse gas fluxes for stormwater detained in a constructed wetland. J Environ Manage 231:1232–1240. https://doi.org/10.1016/j.jenvman.2018.10.106

European Commission (2000) Directive 2000/60/EC of the European Parliament and the Council of 23.10.2000, A framework for community action in the field of water policy,. Off J Eur Communities 71

Fryirs K (2012) (Dis) Connectivity in catchment sediment cascades: a fresh look at the sediment delivery problem. Earth Surf Process Landforms 38:30–46. https://doi.org/10.1002/esp.3242

Gamerith V, Steger B, Hochedlinger M, Gruber G (2011) Assessment of UV/VIS-spectrometry performance in combined sewer monitoring under wet weather conditions. 12th Int Conf Urban Drain 10–15

Gaspar L, Blake WH, Smith HG, Lizaga I, Navas A (2019) Testing the sensitivity of a multivariate mixing model using geochemical fingerprints with artificial mixtures. Geoderma 337:498–510. https://doi.org/10.1016/j.geoderma.2018.10.005

González-Morales D, Valencia A, Díaz-Nuñez A, Fuentes-Estrada M, López-Santos O, García-Beltrán O (2020) Development of a low-cost UV-Vis spectrophotometer and its application for the detection of mercuric ions assisted by chemosensors. Sensors 20:906. https://doi.org/10.3390/s20030906

Guan Z, Tang XY, Yang JE, Ok YS, Xu Z, Nishimura T, Reid BJ (2017) A review of source tracking techniques for fine sediment within a catchment. Environ Geochem Health 39:1221–1243. https://doi.org/10.1007/s10653-017-9959-9

Haddadchi A, Olley J, Laceby P (2014) Accuracy of mixing models in predicting sediment source contributions. Sci Total Environ 497–498:139–152. https://doi.org/10.1016/j.scitotenv.2014.07.105

Haddadchi A, Ryder DS, Evrard O, Olley J (2013) Sediment fingerprinting in fluvial systems: Review of tracers, sediment sources and mixing models. Int J Sediment Res 28:560–578. https://doi.org/10.1016/S1001-6279(14)60013-5

Horowitz AJ (2013) A review of selected inorganic surface water quality-monitoring practices: Are we really measuring what we think, and if so, are we doing it right? Environ Sci Technol 47:2471–2486. https://doi.org/10.1021/es304058q

House WA (2003) Geochemical cycling of phosphorus in rivers. Appl Geochemistry 18:739–748. https://doi.org/10.1016/S0883-2927(02)00158-0

Koiter AJ, Owens PN, Petticrew EL, Lobb DA (2013) The behavioural characteristics of sediment properties and their implications for sediment fingerprinting as an approach for identifying sediment sources in river basins. Earth-Science Rev 125:24–42. https://doi.org/10.1016/j.earscirev.2013.05.009

Kronvang B, Laubel A, Larsen SE, Friberg N (2003) Pesticides and heavy metals in Danish streambed sediment. Hydrobiologia 494:93–101. https://doi.org/10.1023/A:1025441610434

Laceby JP, Evrard O, Smith HG, Blake WH, Olley JM, Minella JPG, Owens PN (2017) The challenges and opportunities of addressing particle size effects in sediment source fingerprinting: A review. Earth-Science Rev 169:85–103. https://doi.org/10.1016/j.earscirev.2017.04.009

Lake NF., Martínez-Carreras N (2021) Data to reproduce the results presented in Lake et al. 2021. Journal of Soils and Sediments, https://doi.org/10.1007/s11368-021-03107-6 ("High frequency un-mixing of soil samples using a submerged spectrophotometer in a laboratory setting – implications for sediment fingerprinting"), Zenodo, Version 1. https://doi.org/10.5281/zenodo.5713544

Lees JA (1997) Mineral magnetic properties of mixtures of environmental and synthetic materials: Linear additivity and interaction effects. Geophys J Int 131:335–346. https://doi.org/10.1111/j.1365-246X.1997.tb01226.x

Martínez-Carreras N (2010) Suspended sediment transport, properties and sources in the Attert River basin (Luxembourg). 196 p

Martínez-Carreras N, Krein A, Udelhoven T, Gallart F, Iffly JF, Hoffmann L, Pfister L, Walling DE (2010a) A rapid spectral-reflectance-based fingerprinting approach for documenting suspended sediment sources during storm runoff events. J Soils Sediments 10:400–413. https://doi.org/10.1007/s11368-009-0162-1

Martínez-Carreras N, Schwab MP, Klaus J, Hissler C (2016) In situ and high frequency monitoring of suspended sediment properties using a spectrophotometric sensor. Hydrol Process 30:3533–3540. https://doi.org/10.1002/hyp.10858

Martínez-Carreras N, Udelhoven T, Krein A, Gallart F, Iffly JF, Ziebel J, Hoffmann L, Pfister L, Walling DE (2010b) The use of sediment colour measured by diffuse reflectance spectrometry to determine sediment sources: Application to the Attert River catchment (Luxembourg). J Hydrol 382:49–63. https://doi.org/10.1016/j.jhydrol.2009.12.017

Mukundan R, Walling DE, Gellis AC, Slattery MC, Radcliffe DE (2012) Sediment source fingerprinting: transforming from a research tool to a management tool. J Am Water Resour 48:1241–1257. https://doi.org/10.1111/j.1752-1688.2012.00685.x

Navratil O, Evrard O, Esteves M, Legout C, Ayrault S, Némery J, Mate-Marin A, Ahmadi M, Lefèvre I, Poirel A, Bonté P (2012) Temporal variability of suspended sediment sources in an alpine catchment combining river/rainfall monitoring and sediment fingerprinting. Earth Surf Process Landforms 37:828–846. https://doi.org/10.1002/esp.3201

Oldfield F, Rummery TA, Thompson R, Walling DE (1979) Identification of suspended sediment sources by means of magnetic measurements: some preliminary results. Water Resour Res 15:211–218. https://doi.org/10.1029/WR015i002p00211

Orlewski PM, Wang Y, Hosseinalipour MS, Kryscio D, Iggland M, Mazzotti M (2018) Characterization of a vibromixer: Experimental and modelling study of mixing in a batch reactor. Chem Eng Res Des 137:534–543. https://doi.org/10.1016/j.cherd.2018.08.003

Owens PN, Batalla RJ, Collins AJ, Gomez B, Hicks DM, Horowitz AJ, Kondolf GM, Marden M, Page MJ, Peacock DH, Petticrew EL, Salomons W, Trustrum NA (2005) Fine-grained sediment in river systems: Environmental significance and management issues. River Res Appl 21:693–717. https://doi.org/10.1002/rra.878

Owens PN, Blake WH, Gaspar L, Gateuille D, Koiter AJ, Lobb DA, Petticrew EL, Reiffarth DG, Smith HG, Woodward JC (2016) Fingerprinting and tracing the sources of soils and sediments: Earth and ocean science, geoarchaeological, forensic, and human health applications. Earth-Science Rev 162:1–23. https://doi.org/10.1016/j.earscirev.2016.08.012

Peart MR, Walling DE (1986) Fingerprinting sediment source: the example of a drainage basin in Devon, UK. In: Drainage basin sediment delivery. IAHS Publication No. 159:41–55

Peart MR, Walling DE (1988) Techniques for establishing suspended sediment sources in two drainage basins in Devon, UK: a comparative assessment. Sediment Budgets, MP Bordas DE Walling (eds), IAHS Publ 174:269–279

Phillips JM, Russell MA, Walling DE (2000) Time-integrated sampling of fluvial suspended sediment: A simple methodology for small catchments. Hydrol Process 14:2589–2602. https://doi.org/

10.1002/1099-1085(20001015)14:14%3c2589::AID-HYP94%3e3.0.CO;2-D

Poulenard J, Legout C, Némery J, Bramorski J, Navratil O, Douchin A, Fanget B, Perrette Y, Evrard O, Esteves M (2012) Tracing sediment sources during floods using Diffuse Reflectance Infrared Fourier Transform Spectrometry (DRIFTS): A case study in a highly erosive mountainous catchment (Southern French Alps). J Hydrol 414–415:452–462. https://doi.org/10.1016/j.jhydrol.2011.11.022

Prairie MW, Frisbie SH, Rao KK, Saksri AH, Parbat S, Mitchell EJ (2020) An accurate, precise, and affordable light emitting diode spectrophotometer for drinking water and other testing with limited resources. PLoS One 15:e0226761. https://doi.org/10.1371/journal.pone.0226761

Pulley S, Rowntree K (2016) The use of an ordinary colour scanner to fingerprint sediment sources in the South African Karoo. J Environ Manage 165:253–262. https://doi.org/10.1016/j.jenvman.2015.09.037

Sequoia Scientific I (2018) LISST-200X Users Manual

Smith HG, Blake WH (2014) Sediment fingerprinting in agricultural catchments: a critical re-examination of source discrimination and data corrections. Geomorphology 204:177–191. https://doi.org/10.1016/j.geomorph.2013.08.003

Smith TB, Owens PN (2014) Flume- and field-based evaluation of a time-integrated suspended sediment sampler for the analysis of sediment properties. Earth Surf Process Landforms 39:1197–1207. https://doi.org/10.1002/esp.3528

Stock BC, Jackson AL, Ward EJ, Parnell AC, Phillips DL, Semmens BX (2018) Analyzing mixing systems using a new generation of Bayesian tracer mixing models. PeerJ 2018:1–27. https://doi.org/10.7717/peerj.5096

Stock BC, Semmens BX (2016) MixSIAR GUI User Manual. Version 3.1. https://github.com/brianstock/MixSIAR.

Tang Q, Fu B, Wen A, Zhang X, He X, Collins AL (2019) Fingerprinting the sources of water-mobilized sediment threatening agricultural and water resource sustainability: Progress, challenges and prospects in China. Sci China Earth Sci 62:2017–2030. https://doi.org/10.1007/s11430-018-9349-0

Thomas MF, Azema N, Thomas O (2017) Physical and aggregate properties. Thomas, O, Burgess, C (Eds) UV-visible spectrophotometry water wastewater Elsevier, 2017

Upadhayay HR, Lamichhane S, Bajracharya RM, Cornelis W, Collins AL, Boeckx P (2020) Sensitivity of source apportionment predicted by a Bayesian tracer mixing model to the inclusion of a sediment connectivity index as an informative prior: Illustration using the Kharka catchment (Nepal). Sci Total Environ 713:136703. https://doi.org/10.1016/j.scitotenv.2020.136703

Vercruysse K, Grabowski RC (2019) Temporal variation in suspended sediment transport: linking sediment sources and hydro-meteorological drivers. Earth Surf Process Landforms 44:2587–2599. https://doi.org/10.1002/esp.4682

Vercruysse K, Grabowski RC, Rickson RJ (2017) Suspended sediment transport dynamics in rivers: Multi-scale drivers of temporal variation. Earth-Science Rev 166:38–52. https://doi.org/10.1016/j.earscirev.2016.12.016

Walling DE, Collins AL (2008) The catchment sediment budget as a management tool. Environ Sci Policy 11:136–143. https://doi.org/10.1016/j.envsci.2007.10.004

Walling DE, Woodward JC (1992) Use of radiometric fingerprints to derive information on suspended sediment sources. In: Erosion and sediment monitoring programmes in river basins. IAHS Publication No. 210:153–243

Walling DE, Woodward JC, Nicholas AP (1993) A multi-parameter approach to fingerprinting suspended-sediment sources. Tracers in Hydrology IAHS Publication No 215:329–338

Wilson HF, Saiers JE, Raymond PA, Sobczak WV (2013) Hydrologic drivers and seasonality of dissolved organic carbon concentration, nitrogen content, bioavailability, and export in a forested New England stream. Ecosystems 16:604–616. https://doi.org/10.1007/s10021-013-9635-6

Wohl E, Bledsoe BP, Jacobson RB, Poff NL, Rathburn SL, Walters DM, Wilcox AC (2015) The natural sediment regime in rivers: Broadening the foundation for ecosystem management. Bioscience 65:358–371. https://doi.org/10.1093/biosci/biv002

Wynants M, Millward G, Patrick A, Taylor A, Munishi L, Mtei K, Brendonck L, Gilvear D, Boeckx P, Ndakidemi P, Blake WH (2020) Determining tributary sources of increased sedimentation in East-African Rift Lakes. Sci Total Environ 717:137266. https://doi.org/10.1016/j.scitotenv.2020.137266